Enhanced embedded system for various synthetic electrocardiogram generation using McSharry's dynamic equation

Nada Fitrieyatul Hikmah, Rachmad Setiawan, Nafila Cahya Andanis, Aldo Pranata
Department of Biomedical Engineering, Faculty of Intelligent Electrical Technology and Informatics,
Institut Teknologi Sepuluh Nopember, Surabaya, Indonesia

Article Info

ABSTRACT

An electrocardiogram (ECG) is a signal that describes the heart's electrical activity. Signal processing techniques are necessary to extract meaningful information from ECG signals. Researchers often use large databases like the PhysioNet database to evaluate the performance of algorithms. However, these databases have limitations concerning the lack of temporal or morphological variations. This study addresses this limitation by introducing a synthetic ECG capable of producing both normal 12-lead ECG signals and abnormal ECG signals and implementing it into the microcontroller. The primary contribution involves developing a synthetic ECG model using McSharry's dynamic equation model and implementing it using Mikromedia 5 for STM32F4 Capacitive as a microcontroller. This model enables users to set the desired heart rate and accurately replicates ECG waveforms using parameters a_i, b_i, and θ_i, each determines the peak's magnitude, the peak's time duration, and the angular velocity of the trajectory. The synthetic ECG was evaluated qualitatively and quantitatively, demonstrating waveform similarity to the ECG signals. This study implies that the synthetic ECG model serves as a valuable tool for researchers and practitioners in electrocardiography. It enables the generation of normal and abnormal ECG signals, aiding in algorithm development and potentially enhancing the understanding and diagnosis of heart conditions.

Corresponding Author:

Nada Fitrieyatul Hikmah
Department of Biomedical Engineering, Faculty of Intelligent Electrical Technology and Informatics,
Institut Teknologi Sepuluh Nopember
Surabaya, Indonesia
Email: nadafh@its.ac.id

1. INTRODUCTION

An electrocardiogram (ECG) is a signal that describes the heart's electrical activity that causes the heart to contract and relax. One normal cycle of the ECG represents the atrial depolarization or repolarization and ventricular depolarization or repolarization activity that occurs with each heartbeat. This cycle can be seen from the ECG waveforms labeled P, Q, R, S, and T. To obtain clinically meaningful information from ECG signals, signal processing techniques include the detection of the R peak, QT interval, derivative of heart rate, and respiration rate from the ECG [1]–[3]. The RR interval is the time between the R-peaks and the series of RR intervals known as the RR tachogram. The variability of the RR interval can provide a lot of important information about human physiology. Evaluation of biomedical signal processing algorithms is usually done by applying them to ECG signals in large databases such as the PhysioNet database. However,

PhysioNet has several limitations, including the absence of time or morphological variations [4]. To address this limitation, synthetic ECG is used to generate ECG data that is not commonly available for various reasons. For instance, an example of an abnormal ECG signal is a myocardial infarction (MI) signal. Existing 12-lead ECG databases such as *Physikalisch-Technische Bundesanstalt* (PTB), *Physikalisch-Technische Bundesanstalt eXtended Leads* (PTB-XL), and ST-T database III (STAFF III) also have a class imbalance. For example, the PTB-XL database, one of the databases that has the most MI signal data, has data on 2,685 patients with inferior MI, 354 patients with anterior MI, 201 patients with Lateral MI, and only 17 patients with posterior MI [5]. This applies not only to MI signals, but there are many different abnormal ECG signal symptoms. To facilitate obtaining ECG data, it is necessary to classify the existing ECG signals. This classification is based on the research by Pałczyński *et al.* [6], which categorizes ECG into five main classes and several sub-classes.

McSharry *et al.* [4] created a dynamic model based on three differential equations that can create real ECG signals. Subsequent researchers widely used this model to create synthetic ECG generators, one of which was carried out by Wei *et al.* [7]. The synthesized synthetic ECG was programmed on the microcontroller unit (MCU) with the help of a field programmable gate array (FPGA), digital-to-analog converter (DAC), liquid crystal display (LCD), flash memory, and keypad. The signal was then displayed using LabVIEW so that the user could access and control the waveform of the generated ECG signal. The created ECG generator allowed the user to easily set various parameters such as sampling frequency, mean heart rate, values of amplitude, duration, and peak at each of the P, Q, R, S, and T, which determine the position of each wave, as well as other parameters. The signal shown in this study is just a normal heart signal at different 3-leads [7].

Zhu *et al.* [8] utilized machine learning via the generative adversarial network (GAN) approach to generate synthetic ECG data, notably achieving a loss function of zero faster than other methods. Lee *et al.* [9] leveraged the PTB dataset to create V-lead ECG signals from limb leads using a GAN with R-peak alignment. This approach preserved physiological information and translated time domain ECG into two-dimensional space using ordered time-sequence embedding. The GAN was pair-trained with modified limb II leads and chest leads. Adib *et al.* [10] created synthetic ECGs with the Wasserstein GAN with gradient penalty (WGAN-GP) model, consistently producing beats closer to real beats than the denoising diffusion probabilistic model (DDPM) beats in every instance and metric. Thambawita's research on WaveGAN and Pulse2Pulse demonstrated the potential of GANs in generating realistic synthetic 10-second 12-lead ECGs, with the latter surpassing WaveGAN in generating 121,977 DeepFake normal ECGs [11]. Hazra and Byun [12] introduced SynSigGAN, a novel GAN model capable of autonomously generating synthetic biomedical signals for electrocardiogram, electroencephalogram, electromyogram, and photoplethysmogram. The model exhibited superior performance in comparison to conventional and other GAN models based on evaluation metrics. Bhagwat and Ravikumar [13] employed the mean average precision (MAP) machine learning method to generate diverse morphologies from real ECG records, using polynomials and spline fits in R2 vector space. However, GAN outperformed MAP by 45.9% in terms of computational complexity. Hernandez-Matamoros *et al.* [14] proposed a new method for synthesizing biomedical signals, involving a bidirectional recurrent neural network and a statistical stage. This method could generate five types of biomedical signals, including electrocardiogram, electroencephalogram, ballistocardiogram, photoplethysmogram, and respiratory impedance, and could be trained in both positive and negative time directions. A shared limitation among all machine learning-based synthetic ECGs is that, to generate an ECG signal, they must initially acquire knowledge from a database. Inaccuracies in the database will consequently lead to inaccuracies in the synthetic ECGs. Moreover, the synthetic ECGs tend to replicate the characteristics of the training signals. For instance, if the training data consists of normal ECG waves, the resulting synthetic ECGs will exhibit normal patterns and will not include any abnormal ECG waves. To incorporate abnormalities, it is essential to have these variations represented in the database for machine learning to learn and replicate them.

Quiroz-Juárez *et al.* [15] employed four mathematical models, including heterogeneous nonlinear oscillators, reaction-diffusion model spatially discretized, differential equations with time delays, and quasi-periodic motion. Parameter adjustments for other ECG patterns are challenging due to the complex parameters. Cheffer *et al.* [16] developed a mathematical model using three nonlinear oscillators with time-delayed connections to describe heartbeats, generating synthetic ECGs for normal and pathological rhythms. However, their focus is on specific arrhythmias, such as atrial flutter, atrial fibrillation, and ventricular fibrillation. Quiroz-Juárez *et al.* [17] proposed a model with two RLC linear oscillators representing the atria and ventricles, along with an electrical cardiac conduction system. Their model addresses only healthy synthetic ECG signals, without studying the parameter effects. Awal *et al.* [18] introduced a simplified model for generating various cardiac dysrhythmias, including normal beats, atrial premature beats, paced beats, and premature ventricular contractions. The model can represent asymmetric ECG components but is limited to specific cases. Que *et al.* [5] developed a dynamic model to generate 12-lead ECGs for myocardial infarction (MI) with

different characteristics, achieving a 95.6% average fidelity using the DTW-GRA distance algorithm. However, the model has yet to validate the similarity to real infarct ECGs.

Thaurisingham et al. [19] devised a model to predict RR intervals employing a time-varying chaotic sequence and an enhanced logistic map multiplied by a constant parameter. They integrated mean heart rate and solved ordinary differential equations; however, their application was limited to healthy patients. Quiroz-Juárez et al. [20] proposed a model for generating electrocardiogram signals through a discretized reaction-diffusion system. This approach utilized three nonlinear oscillators to emulate heart pacemakers, with the ability to control the transition from a normal rhythm to ventricular fibrillation (VF) with a single parameter. While this model eliminated the necessity for multiple parameters or external signals to replicate chaotic heart rhythms, it did not encompass the generation of abnormal ECG waveforms. Bachi et al. [21] developed a simulator based on a discrete-time Markov chain model to simulate atrial and ventricular arrhythmias, with a particular focus on analyzing atrial fibrillation. The simulator incorporated statistical information regarding episode duration, heartbeat characteristics, muscle noise, motion artifacts, and the influence of respiration, making it suitable for data augmentation in machine learning. One limitation of this simulator is its digital representation, as the mathematical model is inherently more complex due to the involvement of multiple parameters, and the output data remains in digital format. Evaristo et al. [22] applied the McSharry model to generate ECG signals, transitioning from a Gaussian model to an autoregressive model for RR tachograms. However, the parameters governing this transition were not adaptable, thereby limiting their capacity to generate abnormal signals. Despite being closer to reality than the Gaussian model, the RR tachograms were solely generated using normal parameters.

Building upon prior research, this study has developed a synthetic ECG capable of generating normal heart signal patterns across 12 leads as well as various heart signals featuring ECG abnormalities categorized in previous ECG classifications. Beyond diversifying the array of heart signal types, this synthetic ECG system allows users to easily adjust heart rate parameters. The synthesis of ECG data was achieved through the utilization of Mikromedia 5, integrated into the STM32F407ZG capacitor, equipped with the STM32F4 microcontroller and visual thin film transistor (TFT). Visual TFT, employing thin-film transistor technology for pixel control, offers the distinct advantage of rendering clearer, sharper, and more vibrant images. The entire program is embedded within the microcontroller, and the resulting synthetic ECG signal is presented via visual TFT. Users can configure heart rate parameters and manipulate the ECG signal waveform through the touchscreen functionality provided by visual TFT. Additionally, in addition to being displayed on visual TFT, the signal is converted into analog form using a digital-to-analog converter via the DAC Click module. In the development of this synthetic ECG, the differential equation framework established by McSharry et al. [4] was employed, with the computational method implemented being Runge-Kutta order 4. The primary contribution of this work lies in the creation of a synthetic ECG model that will serve as a novel dataset. By using synthetic data, this dataset addresses privacy concerns, as traditional ECG datasets are often kept private for confidentiality reasons.

2. METHOD

The synthetic ECG system consists of hardware and software systems. The hardware system uses Mikromedia 5 for STM32 Capacitive, equipped with the STM32F407ZG microcontroller and TFT display. The overall diagram of the synthetic ECG signal generation process can be seen in Figure 1. The heart rate in beats per minute (bpm) and the type of signal to be shown, including normal heart signals at 12-leads and MI signals, were entered into the synthetic ECG. The production of the power spectrum, which is impacted by respiratory sinus arrhythmia (RSA) and Mayer waves, uses temporal and spectral parameters, such as frequency, standard deviation of low frequency (LF) and high frequency (HF), and the ratio of LF to HF.

Mikromedia 5 for STM32 Capacitive is used as the hardware, and the process will operate on the microcontroller STM32F407ZG with visual TFT as a graphic user interface (GUI) for users to enter input heart rate and control signal output. The touchscreen capability on the visual TFT also makes it clear for users to choose and modify the signal output. In addition to the signal displayed via the TFT, the signal is also converted to analog via a digital-to-analog converter (DAC) using DAC Click. The analog signal that comes out through the DAC Click already has a smooth output signal, so there is no need to do a low-pass filter again. A differential voltage divider lowers the signal's voltage once it has been converted to analog.

2.1. RSA and Mayer waves generation

The autonomic nervous system plays a vital role in the regulation of the body's visceral functions by means of the sympathetic and parasympathetic nervous systems. These systems are responsible for maintaining the dynamic equilibrium and essential functions of the body. Within the cardiovascular system, this equilibrium results in fluctuations in heart rate intervals, a phenomenon known as heart rate variability

(HRV) [23]. The activity of the sympathetic nervous system tends to increase heart rate, whereas the activity of the parasympathetic nervous system tends to lower it. The interplay between these two systems is referred to as sympathovagal balance, and it is believed to be reflected in variations in the cardiac cycle from one beat to the next. Spectral analysis of the RR tachogram is a commonly used method to assess the influence of sympathetic and parasympathetic activity. It distinguishes between two primary frequency components: low frequency (LF), which falls within the range of 0.04-0.15 Hz, and high frequency (HF), within the range of 0.15-0.4 Hz, with the HF peak occurring around 0.25 Hz. Notably, the peaks within the LF range are typically associated with Mayer waves and are approximately at 0.1 Hz. Under normal conditions, Mayer waves are attributed to a combination of factors, including the baroreceptor and chemoreceptor feedback system, centrogenic rhythms in the brainstem with connections to respiratory oscillations, and autorhythmicity of vascular smooth muscle [24].
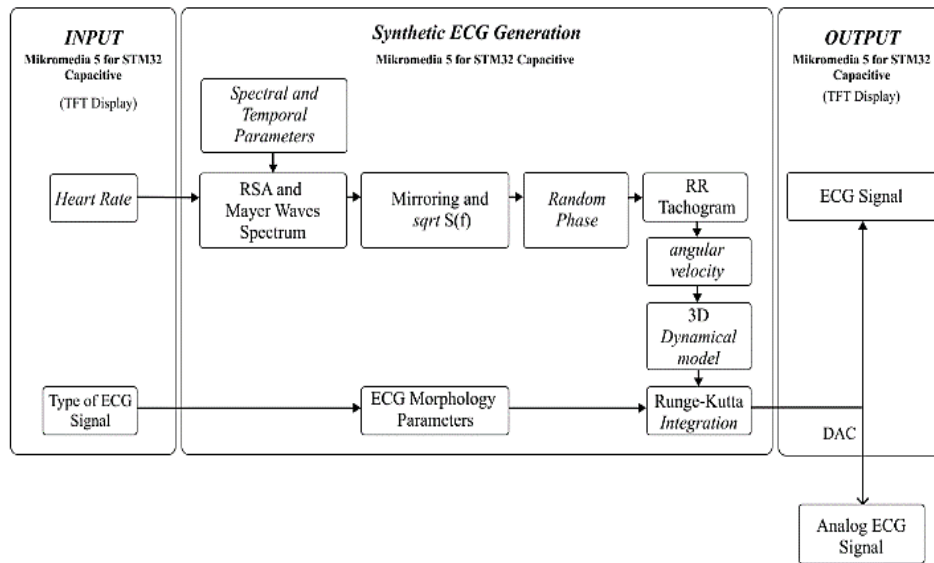

Figure 1. Synthetic ECG system diagram

The effect of RSA and Mayer waves on the $S(f)$ power spectrum on the RR interval can be produced by the sum of the two Gaussian distributions, which can be seen in (1),

$$S(f) = \frac{\sigma_1^2}{\sqrt{2\pi c_1^2}} \, exp\left(\frac{(f-f_1)^2}{2c_1^2}\right) + \frac{\sigma_2^2}{\sqrt{2\pi c_2^2}} \, exp\left(\frac{(f-f_2)^2}{2c_2^2}\right) \tag{1}$$

where variable f_1 and f_2 represent the frequencies of LF and HF, c_1 and c_2 represent the standard deviation of LF and HF respectively, σ_1^2 and σ_2^2 represent the power of LF and HF. While the variation is the same as the total area, it can be written as $\sigma^2 = \sigma_1^2 + \sigma_2^2$, yielding the LF/HF ratio obtained from σ_1^2/σ_2^2. In this research, the initial value $f_1 = 0.1$, $f_2 = 0.25$, $c_1 = 0.01$, $c_2 = 0.01$, dan $\sigma_1^2/\sigma_2^2 = 0.5$ is used.

2.2. RR Tachogram generation

The time series of the RR interval, $T(t)$, with the power spectrum $S(f)$ can be obtained using the inverse discrete Fourier transform (IDFT) method. However, mirroring $S(f)$ is required before applying this technique. According to a study by McSharry *et al.* [4] the amplitude was converted to $\sqrt{S(f)}$ and then given a random phase that was dispersed between 0 and 1 Hz. The signal is initially divided into real and imaginary portions in order to do this random phase operation. The IDFT procedure can then be used to transform frequency-domain signals into time-domain signals. The results of the previous signal, which has been given a random phase, will be used for the IDFT process for each real and imaginary part. The IDFT was followed by the formation of the RR tachogram. In order to create a 3D path later on, the angular velocity from the time series can be obtained by using the formula $\omega(t) = 2\pi/T(t)$ where $T(t)$ is the time series of the RR interval.

2.3. Dynamical model

A three-dimensional path with x, y, and z coordinates is generated by this model. One RR interval or heart rate is represented by each revolution of this trajectory cycle. The quasi-periodicity of the ECG is reflected by the movement of the track around the cycle in the x and y planes. Variations in ECG morphology are formed by movement on a trajectory in the z-direction. The locations of P, Q, R, S, and T are determined by the angles in the cycle named θ_p, θ_Q, θ_R, θ_S, and θ_T. Each point's amplitude is determined by the a and each wave phase's duration is determined by the b. This dynamical model consists of three differentials equations as written in (2),

$$\dot{x} = \alpha x - \omega y$$
$$\dot{y} = \alpha y + \omega x$$
$$\dot{z} = -\sum_{i \in \{P,Q,R,S,T\}} a_i \Delta\theta_i \exp\left(-\frac{\Delta\theta_i^2}{2b_i^2}\right) - (z - z_o) \tag{2}$$

where $\alpha = 1 - \sqrt{x^2 + y^2}$, $\Delta\theta_i = (\theta - \theta_i) mod 2\pi$, $\theta = atan2(y,x)$ and ω is the angular velocity of the track moving during the cycle. Baseline wander is written z_o and plugged into the equation. The phenomenon of baseline wander is noise that frequently appears in ECG readings. The baseline wander equation is written as shown in (3),

$$z_o(t) = A \sin(2\pi f_2 t) \tag{3}$$

where $A = 0.15$ mV. The above equations are integrated numerically using the fourth-order Runge-Kutta method with a fixed-time step $\Delta t = 1/f_s$ where f_s is the sampling frequency. The shape of the ECG signal is influenced by the size of the average heart rate value (h_{mean}). As the heart rate rises, the width of the QRS narrows. Changes caused by heart rate are made by modifying the exponential width and the angular position, which can be seen in Table 1 [25]. The value of α itself can be seen in (4),

$$\alpha = \sqrt{h_{mean}/60} \tag{4}$$

where α is the modulation factor.

Table 1. Parameters of normal ECG morphology with α modulation

Index (i)	P	Q	R	S	T-	T+
Time (secs)	-0.2√α	-0.05α	0	0.05α	0.277√α	0.286√α
θ_i (radians)	$-\frac{\pi\sqrt{\alpha}}{3}$	$-\frac{\pi\sqrt{\alpha}}{12}$	0	$\frac{\pi\alpha}{12}$	$\frac{5\pi\sqrt{\alpha}}{9} - \frac{\pi\sqrt{\alpha}}{60}$	$\frac{5\pi\sqrt{\alpha}}{9}$
a_i	0.8	-5.0	30.0	-7.5	$0.5\alpha^{2.5}$	$0.75\alpha^{2.5}$
b_i	0.2α	0.1α	0.1α	0.1α	$0.4\alpha^{-1}$	0.2α

2.4. 4th order Runge-Kutta

Runge-Kutta is a numerical method commonly used to solve differential equations. The higher the order of Runge-Kutta, the higher the accuracy given, but the more complex the calculation. In this study, the fourth-order Runge-Kutta method was used to integrate the differential equations that were made previously in (2). Runge-Kutta calculations can be carried out as in (5),

$$K_1 = hf(x_n, y_n)$$
$$K_2 = hf(x_n + \frac{1}{2}h, y_n + \frac{1}{2}K_1)$$
$$K_3 = hf(x_n + \frac{1}{2}h, y_n + \frac{1}{2}K_2)$$
$$K_4 = hf(x_n + h, y_n + K_3)$$
$$y_{n+1} = y_n + \frac{1}{6}(K_1 + 2K_2 + 2K_3 + K_4) \tag{5}$$

where K_1, K_2, K_3, and K_4 are Runge-Kutta coefficients, h is step size, x is input, y is output, and n is sequence.

2.5. DAC and differential voltage divider

DAC Click is the device utilized in this study to convert digital signals to analog. DAC Click is a 12-bit digital-to-analog converter MCP4921 which is a product produced by Microelectronics. One of the characteristics of the DAC Click module is its capacity to produce extremely high precision with little noise.

This eliminates any steps in the signal output from the DAC Click, negating the need for a low-pass filter (LPF) circuit. DAC Click is a 12-bit digital-to-analog converter. It means, it has a 12-bit resolution and can output an analog output in a value range of 0-4095. The maximum voltage that can be given by DAC Click or the output voltage value when it is at 4,095 is 3.3 volts. Given that the DAC Click only has an output voltage range from 0 to 3.3 V, the first step in converting digital signals into analog is to add the greatest negative value to all other values to ensure that none of the signal values are negative. The next step is to multiply each ECG signal value by a scaling factor set by (6).

$$Scale = 4,095/maxVal \tag{6}$$

The signal's maximum value is represented by $maxVal$. Therefore, the DAC values that will be output as voltage will be as described by (7).

$$dacVal = Vo * scale \tag{7}$$

A differential voltage divider circuit can be used to reduce the voltage. In this study, the output signal is converted to a differential signal by measuring the voltage difference between points 1 and 2 [26].

3. RESULTS

Signal generation initially took place within the Mikromedia 5 for STM32 Capacitive platform using MikroC Pro for ARM. MikroC Pro for ARM was utilized after the entire signal generation system and variations for different signal types were successfully developed. This platform was chosen due to its robust integration with ARM-based microcontrollers and ability to handle complex signal processing tasks efficiently. By leveraging MikroC Pro's extensive libraries and user-friendly interface, the development process was streamlined, allowing for the creation of versatile and precise signal outputs.

3.1. Signal generation

The outcomes of the spectrum creation in the LF and HF frequencies brought on by RSA events and Mayer waves are depicted in Figure 2. In Figure 2(a), the x-axis represents frequency in Hz units, and the y-axis represents power. The figure shows that LF has a frequency of 0.1 Hz and HF has a frequency of 0.25 Hz. This spectrum's generation was successful because it followed the methodology that was employed. The process of reflecting the signal comes next after this spectrum has been successfully created, as shown in Figure 2(b).

The process of forming the RR tachogram is carried out by continuing the previous process. The signal resulting from mirroring in the previous stage is carried out by the IDFT process. However, it is important to first add a random phase before doing IDFT, the results are shown in Figure 3(a). Once successful, the IDFT procedure can be used. To make the range of RR interval values tolerable at this point, offset values must be included. The RR tachogram will oscillate around 0 seconds prior to adding the offset, thus an offset is carried out, which is the outcome of dividing the input heart rate by 60. The results of the RR tachogram after adding the offset value can be seen in Figure 3(b).
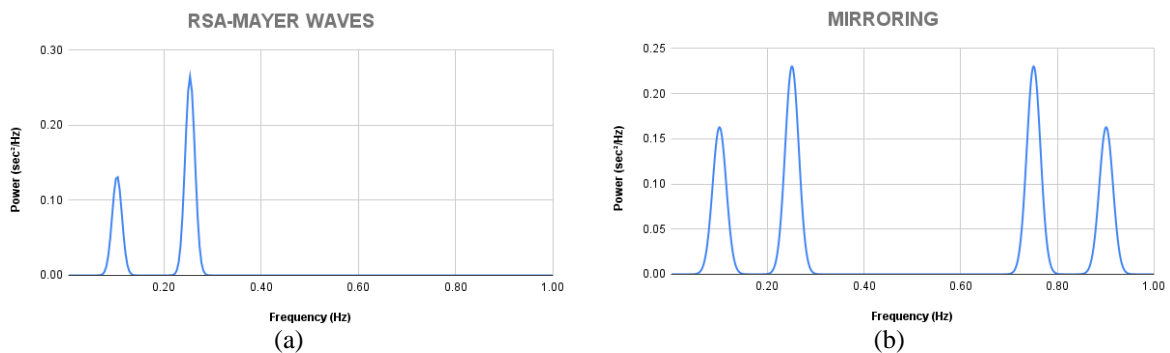

Figure 2. ECG signal generation in frequency domain of (a) LF and HF spectrums and (b) mirroring signal result

(a)   (b)
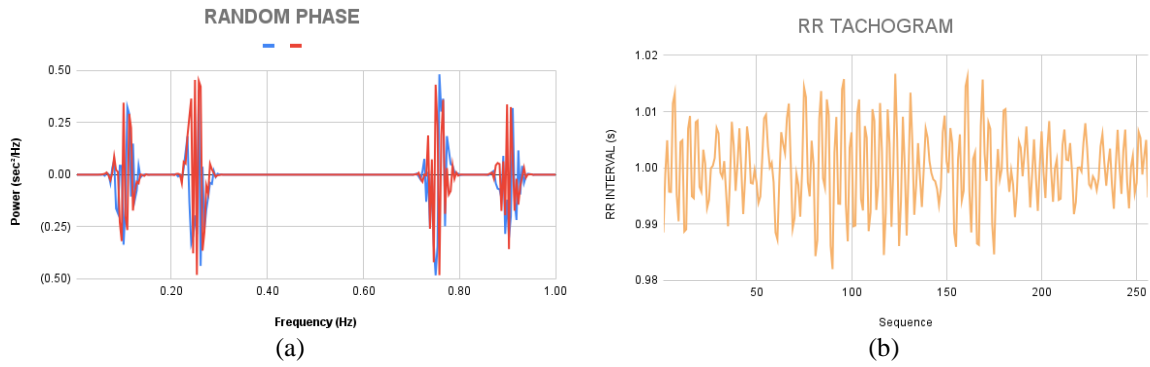
Figure 3. IDFT process in (a) addition of random phases, real (blue), imagery (red) and
(b) RR tachogram after offset (60 bpm)

The ECG signal is formed using the dynamical model equations written in (2). The omega produced in the previous phase is utilized in this equation. In addition, the values of a_i, b_i, and θ_i for each wave is required in order to build the ECG signal's shape. Additionally, the fourth-order Runge-Kutta method, as given in (5), is used to integrate the differential equation in (2).

In this section, one sample is selected from each class of abnormal ECG, and the associated tables and results are presented as depicted in Figure 4. The abnormality of hypertrophy in the ECG signal is shown in Figure 4(a) as left ventricular hypertrophy (LVH). In Figure 4(b), ECG is depicted as lateral myocardial infarction (LMI). In order to generate signals in different ECG formats, the method employed involves varying the ECG parameters listed in Table 2 to configure the desired signal patterns. The parameters in Table 2 have been derived from the modified original ECG signal parameters presented in Table 1. In Table 2, the values for time and θ_i remain unchanged, as the resultant ECG data will not exhibit any changes in the angular velocity of its trajectory. For the LVH data, the magnitude of the parameter a_i in the T- and T+ segments have been inverted to negative, resulting in the inversion of the T signal morphology. In the LMI data, the a_i values for the P, Q, R, and S segments have been adjusted to yield a smaller P wave morphology, a positive Q wave, a negative R wave, and a zero S wave to create ECG data resembling the LMI signal in Lead II.
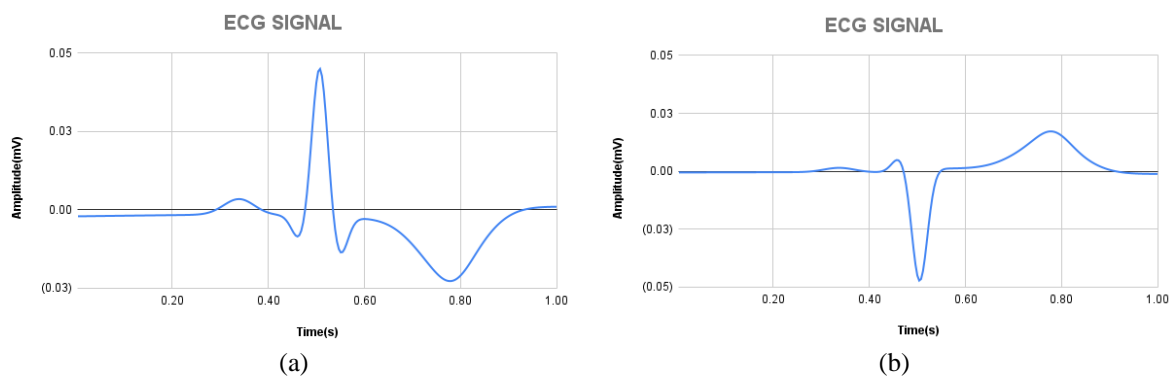

(a)   (b)

Figure 4. ECG synthetic (a) LVH on lead V5 and (b) LMI on lead V2

Table 2. Parameters of LVH and LMI

Index (i)	LVH						LMI					
	P	Q	R	S	T-	T+	P	Q	R	S	T-	T+
Time (secs)	$-0.2\sqrt{\alpha}$	-0.05α	0	0.05α	$0.277\sqrt{\alpha}$	$0.286\sqrt{\alpha}$	$-0.2\sqrt{\alpha}$	-0.05α	0	0.05α	$0.277\sqrt{\alpha}$	$0.286\sqrt{\alpha}$
θ_i (radians)	$-\dfrac{\pi\sqrt{\alpha}}{3}$	$-\dfrac{\pi\sqrt{\alpha}}{12}$	0	$\dfrac{\pi\alpha}{12}$	$\dfrac{5\pi\sqrt{\alpha}}{9} - \dfrac{\pi\sqrt{\alpha}}{60}$	$\dfrac{5\pi\sqrt{\alpha}}{9}$	$-\dfrac{\pi\sqrt{\alpha}}{3}$	$-\dfrac{\pi\sqrt{\alpha}}{12}$	0	$\dfrac{\pi\alpha}{12}$	$\dfrac{5\pi\sqrt{\alpha}}{9} - \dfrac{\pi\sqrt{\alpha}}{60}$	$\dfrac{5\pi\sqrt{\alpha}}{9}$
a_i	0.8	-5.0	30.0	-7.5	$-0.5\alpha^{2.5}$	$-0.75\alpha^{2.5}$	0.3	4.0	-30.0	0	$0.5\alpha^{2.5}$	$0.75\alpha^{2.5}$
b_i	0.2α	0.1α	0.1α	0.1α	$0.4\alpha^{-1}$	0.2α	0.2α	0.1α	0.1α	0.1α	$0.4\alpha^{-1}$	0.2α

3.2. ECG signal on visual TFT

The subsequent phase involves the transfer of all generated signals to the Mikromedia 5 for the STM32 Capacitive platform following their successful creation within the Delphi software. Programming of the Mikromedia 5 for STM32 Capacitive is achieved through MikroC Pro for ARM. The procedures align with the design process for ECG signal generation in software. Each output signal from every step is preconfigured to ensure that each stage yields the appropriate signal output. To facilitate the uploading of programs created in MikroC Pro for ARM into Mikromedia 5 for STM32 Capacitive, an additional tool known as CODEGRIP Suite is required. In this study, the user interface comprises 8 screens. The initial screen prompts the user to specify the heart rate value in beats per minute (bpm) and select the desired signal to be generated. The results of the signal generation on the visual TFT display are depicted in Figure 5(a).

3.3. USB UART Click

USB UART is used in this study to transmit serial data from the resulting synthetic signal to the USART terminal. This serial signal data is being sent with the intention of being stored in a text file and used for additional purposes, one of which is signal testing with other programs. Numerous parameters, such as ComPort, Baud Rate, and others, need to be configured in order to use USB UART Click. The log is used to choose a file to be used as data storage to store serial data produced by synthetic signals. The data storage process can then be started by selecting start logging.

3.4. DAC Click

The next step is to convert the digital signal into analog signal form. DAC Click was initialized on MikroC Pro for ARM and placed on Microbus 1 on the Mikromedia 5 Capacitive Shield. The digital signal data must then be transformed into an analog signal with a similar form after initialization. DAC Click is a 12-bit digital-to-analog converter. This means it has a 12-bit resolution and can output analog output in the value range of 0 to 4,095. The maximum voltage that can be issued by DAC Click or the output voltage value when it is at 4,095 is 3.3 volts. With a high 12-bit resolution, DAC Click is able to issue a smooth signal. The output voltage's DAC must be set to a value range of 0 to 4,095 before converting the signal to analog form. The highest negative signal value is added to the signal first. The signal is then multiplied by the scale value that is produced by dividing 4,095 by the maximum signal value.

3.5. Differential voltage divider circuit

The DAC Click signal will then be lowered in voltage using a differential voltage divider. The signal generation is shown in the condition of the Lateral MI signal on lead V2, which is shown in Figure 5(b). A change in signal amplitude has discernible implications. Reduction of resistance on R2 corresponds to a decrease in the voltage of the output signal, accompanied by an increase in noise. Conversely, an increase in the resistance of R2 leads to a higher voltage on the output signal and a reduction in signal noise. The magnitude of this effect is susceptible to diverse noise sources, both internal, such as thermal noise, and external, such as electromagnetic interference emanating from electronic devices. Each resistor introduces thermal noise, and as resistance decreases within the circuit, current flow intensifies, contributing to elevated thermal noise, subsequently manifesting as increased noise on the oscilloscope. External noise factors, including electronic interference, further influence this behavior.
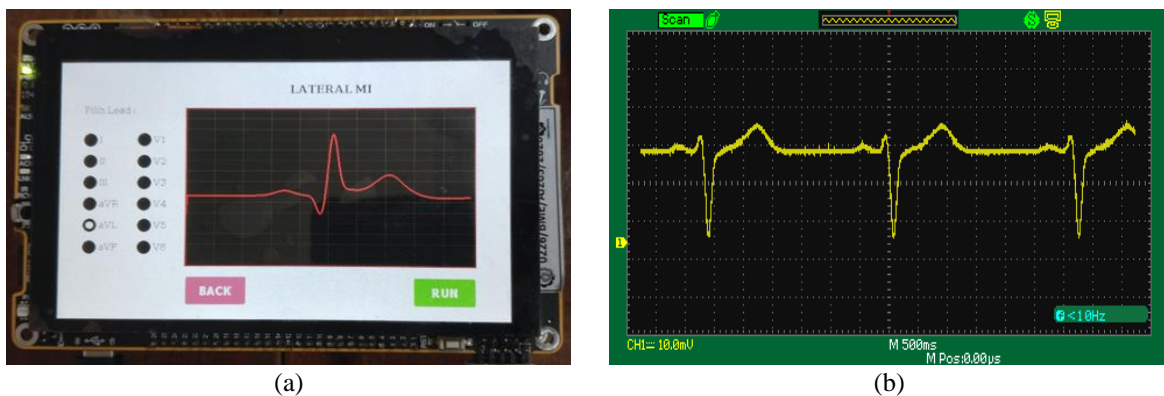

(a)   (b)

Figure 5. Lateral signal MI (a) lead aVL on Mikromedia 5 and (b) lead V2 on DAC

3.6. Quantitative validation

Quantitative validation is conducted by comparing the desired heart rate values with the actual heart rate values. The actual heart rate values are calculated using the Pan-Tompkins method [1]. The heart rates, measured in beats per minute, are set from 40 to 140 in increments of 20. These values are then compared to those obtained through the Pan-Tompkins method. The comparative results are displayed in Table 3. The root mean square error (RMSE) is calculated for these values, yielding a result of 0.02557. This indicates that the produced heart rate values are very similar to the desired values.

Table 3. Comparison between desired and actual heart rate

Desired heart rate (BPM)	Actual heart rate (BPM)
60	59.88
80	79.79
100	99.74
120	120
140	139.64

4.   DISCUSSION

This study introduces a tool for generating synthetic ECG signals, specifically encompassing five distinct classes: normal, hypertrophy, myocardial infarction, ST/T change, and conduction disturbance. The provision of these ECG signals holds significant value, catering to the essential research in ECG signal processing, which necessitates access to comprehensive datasets. The proposed tool offers users the flexibility to set their desired heart rate and select from these signal conditions, enabling the generation of a variety of signal types. Furthermore, the resulting signals will be presented on the visual TFT and are adaptable for utilization in both digital and analog formats on an oscilloscope. This tool serves as a valuable resource for educational purposes, research endeavors, and the provision of ECG signal datasets.

Testing is carried out in stages, starting from testing the system for carrying out signal generation to testing the hardware used. In testing the signal generation system, the RSA spectrum and Mayer waves are first formed using the sum of the two Gaussian equations. The results issued are in accordance with the LF and HF frequencies, as shown in Figure 2(a). After that, mirroring is performed, the results of which are in Figure 2(b), and a random phase is added in the range 0-1 Hz, as shown in Figure 3(a). In this section, the signal is divided into two parts, namely real and imaginary. The results obtained are also in accordance with what should be. To convert the frequency domain into the time domain, the IDFT process is carried out and at this point, the RR tachogram has been formed, as can be seen in Figure 3(b). The RR tachogram test is carried out by varying the heart rate input. The result is that the greater the heart rate entered, the smaller the average RR interval, which means that the distance from R to R is also getting closer. After the RR tachogram is declared appropriate, it can proceed to the next stage, namely modeling the ECG trajectory with a dynamic model. At this stage, the appropriate parameter values are sought to determine the amplitude, width, and location of each wave phase for each type of signal. The results obtained were then compared with the recorded ECG signal on the reference used. One of the results of this modeling can be seen in Figure 5. To diversify the ECG forms, manipulation of the parameters a_i, b_i, and θ_i is carried out, each of which determines the magnitude of the peaks, the width (time duration) of each peak, and the angular velocity of the trajectory. By altering these parameters, a range of ECG signal shapes are produced, enabling the formation of diverse ECG signal types.

The hardware used includes Mikromedia 5 for STM32 Capacitive, DAC Click, USB UART, CODEGRIP, and a differential voltage divider circuit. The entire system that has been formed is then programmed on Mikromedia 5 for STM32 Capacitive. The hardware was also tested in a number of stages. The TFT visual test is performed by creating eight screens and running the signal on the TFT. TFT visuals showed the signal without issue. Following that, USB UART is used to output the signal serial data. The signal data was correctly stored and transmitted successfully. The next step is to use DAC Click to convert digital signal data into analog. The output signal has good results since the DAC module utilized has low noise performance, eliminating the requirement for an additional circuit to smooth the signal. The output analog signal is observed using an oscilloscope.

After observing, the limitation of this study is that output voltage decreases with decreasing resistance, and the resulting signal has more noise. On the other hand, as resistance increases, the output voltage rises, and the signal becomes more rounded. Under these conditions, the amplitude of the ECG signal cannot resemble the original amplitude because, at a voltage of 1 mV, the signal that appears on the oscilloscope is very small and has a lot of noise, and the signal loses its original waveform. However, for this situation, a differential voltage divider was used, thus the outcome is closer to a real electrocardiogram

signal. The proposed method is compared with several existing methods to illustrate its advantages over the others. These comparisons are presented in Table 4.

Table 4. Comparison with other methods

Name	Method	Result	Limitation	Accuracy of signals
Zhu *et al.* [8]	Machine learning with GAN	Normal ECG	Database needed	RMSE 0.257
Lee *et al.* [9]	GAN with R-peak alignment	V-lead ECG	Database needed	RMSE 0.25-0.35
Thambawita *et al.* [11]	WaveGAN	121.977 DeepFake normal ECG	Database needed	Accuracies from 150.000 deep fakes 81.6% (max)
Hernandez-Matamoros *et al.* [14]	Bidirectional recurrent neural network	Positive and negative time direction ECG	Database needed	Accuracies 93.9% - 99.9%
Quiroz-Juárez *et al* [15]	Heterogeneous nonlinear oscillator. Reaction-diffusion model spatially discretized, differential equation with time delays, and quasi-periodic motion	Various ECG signal	Complex parameter	Not mentioned
Quiroz-Juárez *et al.* [17]	Two RLC linear oscillators	Healthy synthetic ECG	No parameter	Not mentioned
Thaurisingham [19]	Time-varying chaotic sequence and enhanced logistic map	Mean heart rate of ECG	Limited to a healthy patient	Not mentioned
Bachi *et al.* [21]	Simulator-based on a discrete-time Markov chain model	ECG, primarily focuses on atrial fibrillation	Limited to digital representation due to the complex involvement of multiple parameters	Average fitting error 5.4%
Evaristo *et al.* [22]	Applied McSharry dynamic model with autoregressive model for RR tachograms	ECG and RR tachogram	The transition parameter is not adaptable	Not mentioned
Proposed Method	Enhanced McSharry dynamic model	Various ECG signals with flexible parameters, embedded using Mikromedia 5 for user interface, and provide digital-analog data using DAC	The amplitude of the ECG signal cannot resemble the original amplitude when below 1 mV	RMSE 0.02557

As shown in Table 4, methods utilizing neural networks require a database, and the resulting ECG signals will inevitably follow the learning ECG signals derived from the database. This dependency makes it challenging to generate signals with morphologies different from those in the learning signals. In contrast, when compared to other methods that use dynamic equations to produce ECG data, the parameters of the proposed method are simpler and more flexible for generating various types of synthetic ECG data. Most validation methods in related works utilize qualitative approaches, emphasizing the similarity between the morphology of the generated signal and the desired signal. This reliance on qualitative assessment makes subjective comparison between the proposed method and existing methods challenging. Through quantitative comparison, it was found that the similarity between the desired signal and the generated signal using this method has a lower error rate compared to several other methods employing similar quantitative validation techniques. This indicates that the proposed method is more accurate in producing the desired signal. Additionally, this ECG data is stored in both digital and analog formats and embedded in Mikromedia 5, facilitating the ease of use of the device. This implies that the synthetic ECG model from this study may serve as a valuable tool for researchers and practitioners in electrocardiography. It enables the generation of abnormal ECG signals, aiding in algorithm development and evaluation, and potentially enhancing the understanding and diagnosis of heart conditions.

5. CONCLUSION

This study proposed a synthetic ECG generator, created using a dynamical model that can produce a 12-lead signal under various ECG conditions. This model is generated using the parameters a_i, b_i, and θ_i, each of which determines the magnitude of the peaks, the width (time duration) of each peak, and the angular velocity of the trajectory. Subsequently, these signals are implemented on visual TFT hardware to fulfill various requirements. The resulting data comprises both analog and digital ECG data. The research undertaken was assessed through qualitative and quantitative evaluation. The evaluation results indicate that the analog signal observed on the oscilloscope already replicates the waveform of the original signal.

However, it does not yet accurately mimic the actual voltage amplitude. Furthermore, for enhanced precision in the analog signal output, there is a desire to further align the amplitude of the analog signal with the intended amplitude of the ECG signal by utilizing surface mount device (SMD) resistors. SMD resistors exhibit high accuracy owing to their minimal tolerance in comparison to color-coded resistors. It can be deduced that the parameters primarily influencing the morphology of electrocardiogram signals are the parameters a_i, b_i, and θ_i. Future research could explore optimizing these parameters to improve signal accuracy further and investigate other hardware solutions that could enhance signal fidelity. Additionally, the application of this synthetic ECG generator in clinical settings could be examined to determine its practicality and effectiveness in training medical professionals or in diagnostic scenarios. Such advancements could significantly contribute to the field of medical technology and practice.

REFERENCES

[1] N. F. Hikmah, A. Arifin, T. A. Sardjono, and E. A. Suprayitno, "A signal processing framework for multimodal cardiac analysis," in *2015 International Seminar on Intelligent Technology and Its Applications (ISITIA)*, May 2015, pp. 125–130, doi: 10.1109/ISITIA.2015.7219966.

[2] N. F. Hikmah, R. Setiawan, and M. D. Gunawan, "Sleep quality assessment from robust heart and muscle fatigue estimation using supervised machine learning," *International Journal of Intelligent Engineering and Systems*, vol. 16, no. 2, pp. 319–331, Feb. 2023, doi: 10.22266/ijies2023.0430.26.

[3] N. F. Hikmah, R. Setiawan, and T. A. Putri, "Real-time detection of premature ventricular contraction using discrete wavelet transform," in *2022 International Seminar on Intelligent Technology and Its Applications (ISITIA)*, Jul. 2022, pp. 12–17, doi: 10.1109/ISITIA56226.2022.9855271.

[4] P. E. McSharry, G. D. Clifford, L. Tarassenko, and L. A. Smith, "A dynamical model for generating synthetic electrocardiogram signals," *IEEE Transactions on Biomedical Engineering*, vol. 50, no. 3, pp. 289–294, Mar. 2003, doi: 10.1109/TBME.2003.808805.

[5] W. Que, C. Han, X. Zhao, and L. Shi, "An ECG generative model of myocardial infarction," *Computer Methods and Programs in Biomedicine*, vol. 225, Oct. 2022, doi: 10.1016/j.cmpb.2022.107062.

[6] K. Pałczyński, S. Śmigiel, D. Ledziński, and S. Bujnowski, "Study of the few-shot learning for ECG classification based on the PTB-XL dataset," *Sensors*, vol. 22, no. 3, pp. 1–25, Jan. 2022, doi: 10.3390/s22030904.

[7] Y.-C. Wei, Y.-Y. Wei, K.-H. Chang, and M.-S. Young, "A three-lead, programmable, and microcontroller-based electrocardiogram generator with frequency domain characteristics of heart rate variability," *Review of Scientific Instruments*, vol. 83, no. 4, pp. 1–7, Apr. 2012, doi: 10.1063/1.3693278.

[8] F. Zhu, F. Ye, Y. Fu, Q. Liu, and B. Shen, "Electrocardiogram generation with a bidirectional LSTM-CNN generative adversarial network," *Scientific Reports*, vol. 9, no. 1, pp. 1–11, May 2019, doi: 10.1038/s41598-019-42516-z.

[9] J. Lee, K. Oh, B. Kim, and S. K. Yoo, "Synthesis of electrocardiogram V-lead signals from limb-lead measurement using R-Peak aligned generative adversarial network," *IEEE Journal of Biomedical and Health Informatics*, vol. 24, no. 5, pp. 1265–1275, May 2020, doi: 10.1109/JBHI.2019.2936583.

[10] E. Adib, A. S. Fernandez, F. Afghah, and J. J. Prevost, "Synthetic ECG signal generation using probabilistic diffusion models," *IEEE Access*, vol. 11, pp. 75818–75828, 2023, doi: 10.1109/ACCESS.2023.3296542.

[11] V. Thambawita *et al.*, "DeepFake electrocardiograms using generative adversarial networks are the beginning of the end for privacy issues in medicine," *Scientific Reports*, vol. 11, no. 1, pp. 1–8, Nov. 2021, doi: 10.1038/s41598-021-01295-2.

[12] D. Hazra and Y.-C. Byun, "SynSigGAN: generative adversarial networks for synthetic biomedical signal generation," *Biology*, vol. 9, no. 12, pp. 1–20, Dec. 2020, doi: 10.3390/biology9120441.

[13] K. Bhagwat, S. M., and A. Ravikumar, "Map composition framework for synthetic P morphology," *Biomedical Signal Processing and Control*, vol. 79, Jan. 2023, doi: 10.1016/j.bspc.2022.104063.

[14] A. Hernandez-Matamoros, H. Fujita, and H. Perez-Meana, "A novel approach to create synthetic biomedical signals using BiRNN," *Information Sciences*, vol. 541, pp. 218–241, Dec. 2020, doi: 10.1016/j.ins.2020.06.019.

[15] M. A. Quiroz-Juárez, J. A. Rosales-Juárez, O. Jiménez-Ramírez, R. Vázquez-Medina, and J. L. Aragón, "ECG patient simulator based on mathematical models," *Sensors*, vol. 22, no. 15, pp. 1–19, Jul. 2022, doi: 10.3390/s22155714.

[16] A. Cheffer, M. A. Savi, T. L. Pereira, and A. S. de Paula, "Heart rhythm analysis using a nonlinear dynamics perspective," *Applied Mathematical Modelling*, vol. 96, pp. 152–176, Aug. 2021, doi: 10.1016/j.apm.2021.03.014.

[17] M. A. Quiroz-Juárez, O. Jiménez-Ramírez, J. L. Aragón, J. L. Del Río-Correa, and R. Vázquez-Medina, "Periodically kicked network of RLC oscillators to produce ECG signals," *Computers in Biology and Medicine*, vol. 104, pp. 87–96, Jan. 2019, doi: 10.1016/j.compbiomed.2018.05.017.

[18] M. A. Awal *et al.*, "Design and optimization of ECG modeling for generating different cardiac dysrhythmias," *Sensors*, vol. 21, no. 5, pp. 1–26, Feb. 2021, doi: 10.3390/s21051638.

[19] R. A. Thuraisingham, "Generation of synthetic RR interval sequences of healthy patients," *Biomedical Signal Processing and Control*, vol. 77, Aug. 2022, doi: 10.1016/j.bspc.2022.103843.

[20] M. A. Quiroz-Juárez, O. Jiménez-Ramírez, R. Vázquez-Medina, V. Breña-Medina, J. L. Aragón, and R. A. Barrio, "Generation of ECG signals from a reaction-diffusion model spatially discretized," *Scientific Reports*, vol. 9, no. 1, pp. 1–10, Dec. 2019, doi: 10.1038/s41598-019-55448-5.

[21] L. Bachi *et al.*, "ECG modeling for simulation of arrhythmias in time-varying conditions," *IEEE Transactions on Biomedical Engineering*, vol. 70, no. 12, pp. 3449–3460, Dec. 2023, doi: 10.1109/TBME.2023.3288701.

[22] R. M. Evaristo, A. M. Batista, R. L. Viana, K. C. Iarosz, J. D. Szezech Jr, and M. F. de Godoy, "Mathematical model with autoregressive process for electrocardiogram signals," *Communications in Nonlinear Science and Numerical Simulation*, vol. 57, pp. 415–421, Apr. 2018, doi: 10.1016/j.cnsns.2017.10.018.

[23] B. Xhyheri, O. Manfrini, M. Mazzolini, C. Pizzi, and R. Bugiardini, "Heart rate variability today," *Progress in Cardiovascular Diseases*, vol. 55, no. 3, pp. 321–331, 2012, doi: 10.1016/j.pcad.2012.09.001.

[24] S. R. Seydnejad and R. I. Kitney, "Modeling of Mayer waves generation mechanisms: Determining the origin of the low and very low frequency components of BPV and HRV," *IEEE Engineering in Medicine and Biology Magazine*, vol. 20, no. 2, pp. 92–100, 2001, doi: 10.1109/51.917729.

[25] G. D. Clifford, F. Azuaje, and P. E. McSharry, *Advanced methods and tools for ECG data analysis*. Artech House, 2006.

[26] M. Kaczmarek, "Two channels opto-isolation circuit for measurements of the differential voltage of voltage transformers and dividers," *Energies*, vol. 15, no. 7, p. 2694, Apr. 2022, doi: 10.3390/en15072694.

BIOGRAPHIES OF AUTHORS

Nada Fitrieyatul Hikmah earned her bachelor's degree in biomedical engineering from Airlangga University (UNAIR) in 2012. She then pursued her master's education in electrical engineering-electronics, specializing in biomedical engineering, at the Sepuluh Nopember Institute of Technology (ITS) and earned her master's degree in 2016. Currently, she works as a lecturer at the Department of Biomedical Engineering, Faculty of Electrical Technology and Intelligent Informatics, ITS, Indonesia. Her research interests include cardiac engineering, signal processing, and medical imaging. She can be contacted at email: nadafh@bme.its.ac.id.

Rachmad Setiawan earned a bachelor's degree in electronics from the Sepuluh Nopember Institute of Technology (ITS) in 1995. Then continued his masters degree in instrumentation and control at the Bandung Institute of Technology (ITB), and earned his master's degree in 1999. In 2013-2014 he conducted researched the development of closed-loop FES system, with an emphasis on developing system infrastructure, joint angle sensors, and wearable controllers based on wireless technology. His current activity is to become a lecturer at the Department of Biomedical Engineering, Faculty of Intelligent Electrical and Informatics Technology, Sepuluh Nopember Institute of Technology (ITS), Indonesia. He can be contacted at email: rachmad@bme.its.ac.id.

Nafila Cahya Andanis proceeded to a higher level of education to the Department of Biomedical Engineering, Sepuluh Nopember Institute of Technology in 2019. While studying at the Sepuluh Nopember Institute of Technology, the author was active in several activities, some of which were as general secretary at the ITS Robotics UKM, and active as a biomedical instrumentation and signal processing laboratory assistant. She can be contacted at email: nafilacahya@gmail.com.

Aldo Pranata has taken formal education from elementary school education at SDIT Al-Azhar Batam and continued to junior high school at SMP Harapan Utama, then continued to senior high school at SMAN 1 Batam. Then the author proceeded to a higher level of education to the Department of Biomedical Engineering, Sepuluh Nopember Institute of Technology in 2021. He can be contacted at email: aldopranata751@gmail.com.